A MECHANICS-BASED APPROACH FOR PUTT DISTANCE OPTIMIZATION

by

PASCUAL SANTIAGO-MARTINEZ

A thesis submitted in partial fulfillment of the requirements
for the Honors in the Major Program in Mechanical Engineering
in the College of Engineering and Computer Science
and in the Burnett Honors College
at the University of Central Florida
Orlando, Florida

Spring Term, 2015

Thesis Chair: Ali P. Gordon, Ph. D

ABSTRACT

Quantifying the core mechanics of putting is imperative to developing a reliable model that predicts post-collision ball behavior. A preliminary model for the stroking motion of putting and putter-ball collision is developed alongside experiments, establishing an empirical model that supports the theory. The goal of the present study is to develop a correlation between the backstroke of a putt, or the pre-impact translation of the putter, and the post-impact displacement of the golf ball. This correlation is subsequently utilized to generate an algorithm that predicts the two-dimensional ball trajectory based on putt displacement and putting surface texture by means of finite element analysis. In generating a model that accurately describes the putting behavior, the principles of classical mechanics were utilized. As a result, the putt displacement was completely described as a function of backstroke and some environmental parameters, such as: friction, slope of the green, and the elasticity of the putter-ball collision. In support of the preliminary model, experimental data were gathered from golfers of all levels. The collected data demonstrated a linear correlation between backstroke and putt distance, with the environmental parameters factoring in as a constant value; moreover, the data showed that experienced golfers tend to have a constant acceleration through ball impact. Combining the empirical results with the trajectory prediction algorithm will deliver an accurate predictor of ball behavior that can be easily implemented by golfers under most practical applications. Putt distance to backstroke ratios were developed under a variety of conditions

ACKNOWLEDGEMENTS

I would like to thank Dr. Gordon, for providing me the opportunity to do research under his group, providing me the guidance and support to take my work to the next level, and showing me the things that I am capable of achieving with the help of an inspirational leader. I would also like to acknowledge coach Pellicani and the Mike Bender Golf Academy for providing the original project idea and the facilities for data analysis, and Matt Brown for performing the initial phase of the research with me. Lastly, I would like to thank Nicholas Jones for assisting me with the MATLAB code and debugging.

TABLE OF CONTENTS

LIST OF FIGURES

LIST OF TABLES

NOMENCLATURE

$D_B \stackrel{\text{def}}{=}$ Backswing Distance

$D_P \stackrel{\text{def}}{=}$ Desired Putt Distance

$V_0 \stackrel{\text{def}}{=}$ Launch Velocity

$m_p \stackrel{\text{def}}{=}$ Mass of Ball

$a_p \stackrel{\text{def}}{=}$ Putter Acceleration

$F_p \stackrel{\text{def}}{=}$ Putter Force

$L_g \stackrel{\text{def}}{=}$ Stimpmeter Length

$D_g \stackrel{\text{def}}{=}$ Green Speed

$C_g \stackrel{\text{def}}{=}$ Stimpmeter Constant

$V_g \stackrel{\text{def}}{=}$ Stimpmeter Launch Velocity

$\theta_g \stackrel{\text{def}}{=}$ Stimpmeter Angle

$\mu \stackrel{\text{def}}{=}$ Friction Coefficient

$\phi \stackrel{\text{def}}{=}$ Incline of Green

$m \stackrel{\text{def}}{=}$ Slope of Green

$e \stackrel{\text{def}}{=}$ Coefficient of Restitution

$C_c \stackrel{\text{def}}{=}$ Impact Correction Factor

$C_e \stackrel{\text{def}}{=}$ Collision Constant

$m_p \stackrel{\text{def}}{=}$ Mass of Putter

$m_b \stackrel{\text{def}}{=}$Mass of Ball

CHAPTER 1: INTRODUCTION

Currently, golf instruction is primarily conveyed by kinesthetic instruction rather than via concepts of energy, momentum, and kinematics. Current approaches to golf instruction rely heavily on emulating more experienced golfers, and are founded on the idealization of certain styles based on previous performance. Scientific approaches to coaching are generally not utilized because they lack the ease of use that current methods achieve. In light of this observation, there is a need for golf instruction that employs metrics to develop the skill of any player with a consistency inherent to the scientific principles that back them up. It would be greatly advantageous to coaches and players of the sport to have access to such metrics, which would establish a universal foundation for skill development. Additionally, these metrics will provide a new perspective on the sport, allowing for novel approach, building on and improving the current methods of golf instruction.

There have been endeavors to describe the behavior of putting [1, 2], but their aim generally gears towards establishing an empirical correlation between putting parameters like swing speed, backstroke, and putter dimensions. The focus on these undertakings utilizes a number of key assumptions that make the final overall putt distance method simplified; there is no intention of implementing the findings in any real world scenario. The present study aims to utilize these findings to establish a model for a putt and its post-impact ball displacement by identifying the human and environmental parameters that primarily affect it. The relationship between these parameters is founded on scientific derivations, and is developed in a manner that is easily understandable and employable by golfers of all skill levels under most gameplay scenarios, and

with an acceptable degree of consistency. The constraints imparted by these goals progress the generated model from a deterministic model to a more universal, probabilistic model.

The model will be developed by merging three different approaches. First, an analytical model will be developed, which will describe the behavior of putting and develop a relationship between the parameters inherent to it, such as backstroke (D_B), downswing distance or follow through (D_{ds}), ball launch velocity (V_g), surface texture (μ, ϕ), and post-impact ball displacement (D_P). Second, experiments will be performed to corroborate the model and examine the behavior of each parameter in relation to putting and putt distance. Finally, the corroborated model will establish a baseline from which a numerical analysis algorithm will perform prediction on post impact ball displacement.

The following chapters are structured to follow the order in which the putt distance model was developed. Chapter 2 displays the current research in golf and putting that is pertinent to developing a prediction model for putt distance, and accurately describing the importance of each parameter in the putting stroke. Following the background research on putting, Chapter 3 describes the procedure in developing the theoretical model that describes the putting motion and relates the effect of each parameter to post-impact putt displacement. Chapter 4 contains the experimental methods that were pursued in order to corroborate the theoretical model and establish an empirical relationship for the variables inherent to putting. Chapter 5 details the development of the numerical methods that were pursued in order to develop a putt distance prediction model in MATLAB, while Chapter 6 details all of the testing that took place to validate the model, and the results obtained from the testing. Finally, Chapter 7 goes over the developed model and its

findings, while explaining how the model can be applied to the sport of golf and its instruction. Chapter 7 also develops a direction in which the model can be taken, offering improvements to, and further applications of the putting model.

CHAPTER 2: BACKGROUND

In general, a solid scientific analysis in sports is a difficult goal to achieve, and the sport of golf does not deviate from the norm. The mathematics behind the sport are so complex and inclusive of so many variables that an exact prediction model remains inaccessible. With the continuing advances in technology, a higher number of tools have been able to be employed in the analysis of golf and have brought researchers closer to an ideal model that explains the exact behavior of the ball. With improvements in the available technology and software, scientists are able to design tests and gather more data with increasing accuracy, allowing the development of some groundbreaking empirical models and paving the way to discoveries in the behavior of golf, and more particularly, putting [3].

Many researchers endeavor to identify the key differences in the putting motion between novice and expert golfers [1, 2, 4]. The idea is that with analysis of a broad range of variables, some patterns may arise in the data collected that points in the direction of a more consistent, and thusly, predictable behavior in putting. If a well-defined pattern can be established for the putting behavior of the more elite golfers, a reliable empirical model can be created for implementation in the sport.

A common question posed by many researchers in the study of putting, like Sim [2] and Choi [4] is whether there exists a difference in behavior between putters with experience and novices. This was the question driving the research of Sim and Kim [2], who performed an investigation on the kinematics and accuracy of expert and novice golfers. The experiment consisted of the two groups of golfers putting over various distances (1.7m, 3.25m, and 6m) and

with different putter weights (500g and 750g). Experienced golfers were teaching professionals with single-digit handicaps, while novices had no prior golf-putting experience. The kinematics were analyzed by video recording of the putting motion, while the accuracy of the putts was measured by calculating the distance from the target with the distance formula:

$$error = \sqrt{(y' - y)^2 + (x' - x)^2} \tag{2.1}$$

where the point (x, y) denotes the position of the golf ball and (x', y') denotes the position of the target on the putting surface. This, along with stroke duration, stroke amplitude, and stroke velocity, which characterize the kinematics of each putt, enable a deeper understanding of the putting behavior, and aid in establishing the possible fundamental divergence between the putting of golfers of differing skill levels.

Among the main differences between putter groups was the accuracy. The accuracy is shown to be higher for the experienced group, as expected [2]; furthermore, and more interestingly, the data showed that the backstroke length and stroke velocity were both around 30% and 23% smaller, respectively, for the experienced golfers. In addition, the geometry of the stroke was distinct for the two groups, as evidenced by Figure 2.1. In modeling the putter as a pendulum, the stroke of the novices demonstrates greater symmetry between backstroke and follow through, whereas the experts impact the ball (located at the coordinate of y=0) sooner in the stroking motion, at about one third of the total length of the putt. When considering the distance of a putt, Sim and Kim [2] found that the variables with the most correlation to putt distance (D_P) were the backstroke

(D_B) and velocity of the putt (V_P). Despite the weight of the putt and the experience level of the putters, there was always an increase in D_B and V_P as D_P increased.

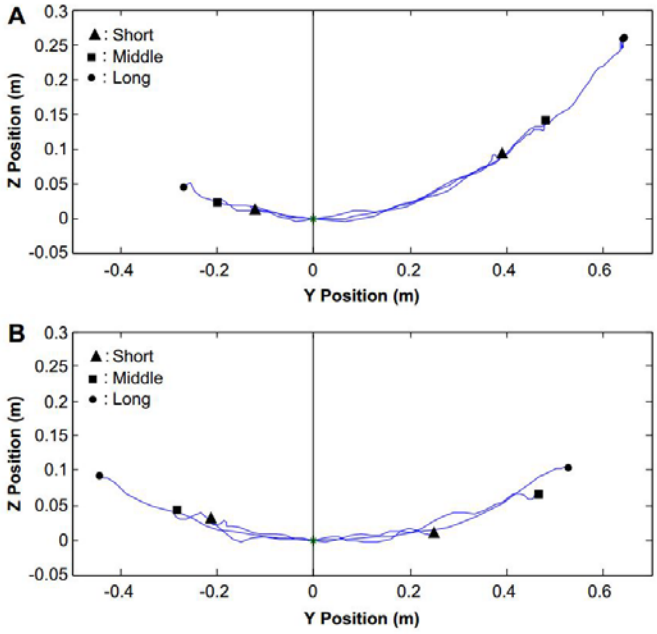

Figure 2.1 - Putting Geometry for Experts (A) and Novices (B) [2]

Similar experiments were performed by Delay et al [1], although the discoveries provided more insight into the putting behavior itself rather than the discrepancies between golfers of differing skill levels. Two groups of golfers were asked to putt to a target located over four distances, 1, 2, 3, and 4 m, respectively. Data were recorded to analyze the behavior of the putt, in a similar manner to the studies performed by Sim and Kim [2]. In accordance with the aforementioned results, the key influential factors with respect to D_P are D_B and V_P.

In contrast to the studies performed by Sim [2], Delay et al [1] places much more emphasis on the individual factors in the putt. One of the variables that he investigates in his studies is what

he calls the downswing, or follow through (D_{ds}). In their studies, Delay et al [1] compare D_{ds} as a function of D_P, and demonstrated a strong correlation between the two. Similar to the backstroke (D_B) of the putt, D_{ds} increases with increasing putt distance; furthermore, the D_{ds} amplitude is generally around three times as much as that of D_B for the more experienced golfers. These results support the data published by Sim and Kim [2], which discusses how the expert golfers impact the ball around a third of the way through the stroke. This allows the golfers to impact the ball with a lower velocity, and follow along with the ball for a slight amount of time, which reduces ball rotation and skipping, thus decreasing the uncertainty of each putt.

Another important result from Delay and co-authors [1] involves the timing of the putts. Data showed that the time to impact for each putt is essentially invariant over every target distance and for all skill levels. Even though the more experienced golfers demonstrate a higher degree of isochrony, described as the consistency in the timing of the putts, and estimated by the equation $V = K + b \log p$, where V represents the mean movement velocity, p is the movement amplitude, and K is a constant [1]. Experts demonstrated a mean isochrony value of 0.9, while novices had a value closer to 0.8. There is little variance in this parameter, demonstrating that golfers of all skill levels adjust their acceleration in accordance with D_B for different D_P, resulting in the same time to impact over all putts.

In the quest for greater insight into the sport, Choi and colleagues [4] decided to give a fresh perspective on putting with their research. Instead of focusing on the previously covered variables of backstroke, follow through, time to impact and putter acceleration, Choi et al [4] set their sights on the actual kinematics of the golfer. With the goal of modeling the motion of the

putter as it swings during a putt, Choi et al [4] observed novice and experienced golfers putt to a target placed at distances of 1, 3, and 5 m. In order to compare the performance of each golfer in terms of human factors, they investigated the smoothness of the putter head motion during a putt for each player. The smoothness of the putting motion can be readily quantified by analyzing the jerk of the putt, through the function:

$$JC(r(t)) = \int_0^T \left(\frac{d^3r}{dt^3}\right)^2 dt \tag{2.2}$$

This function, called the jerk cost function [5] is dependent on the position function, $r(t)$ which is the function that will be captured for the golfers. For the sake of repletion, the jerk cost function is to be analyzed for three different position functions, the anterior-posterior, mediolateral, and vertical directions.

For the two groups, it was found that JC increases as the target distance increases with the same rate for both groups. A significant divergence in the rate of change of the cost function for the two groups only surfaced for the position function in the mediolateral direction, making it the only quantifiable index for the experience level of a golfer. In addition, tracking of the rotational motion of the golfers during the putt, it was found that the motion of the experienced golfers converged to a point, whereas the novice golfers had no exact point of convergence. This discrepancy in the putting motion of the two groups was only exacerbated as the target distance increased.

From their research, Choi et al [4] concluded that the increased smoothness and similarity in putting motion of the more experienced golfers helps their putts be much more predictable;

moreover, the behavior of their putts resemble the motion of a pendulum, which, coupled with their consistency and smooth position function, facilitates the creation of a model that replicates the putter head position and velocity with a higher degree of reliability for the more experienced golfers.

Continuing the work on modeling the putting motion, Penner [6] tackles the problem from an entirely theoretical standpoint. Splitting the putting action into many parts, he performs a rigorous analysis of the theoretical foundation behind the sport. Starting from the fundamental laws of motion, and considering all of the influential environmental parameters in a putting green, Penner [6] develops a two dimensional model of the putting trajectory, as a function of the slope of the green, friction due to the grass cut, and the rotation of the ball. The equations developed, however, only consider the trajectory of the ball after being impacted by the putter.

Another focus of research concerned the stimpmeter and the measurements obtained by it. The stimpmeter is a device, standardized by the USGA, which measures the speed of putting greens. It has a notch in which the ball rests, and is released at an angle of 20^{o} [8, 10]. The ball is released in one direction several times, then the direction is reversed and the measurements are taken a second time [7]. Once measurements are taken in both directions, the average is determined to be the green speed. This approach works well for flat surfaces, but research performed by Brede [9] demonstrated that the arithmetic average introduced error in measurements taken over a sloped surface (see Figure 2.2).

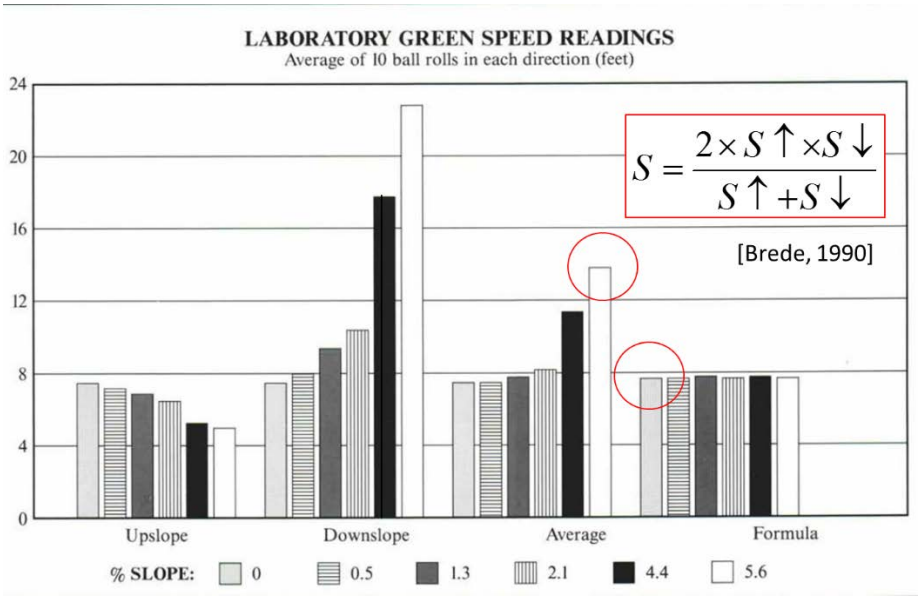

Figure 2.2 - Green Speed Measurements Obtained by Averaging vs. Brede Formula [9]

In order to reduce the averaging error, Brede analyzed the speed of the green up and downhill using Newtonian physics, arriving to the formula

$$S = \frac{2S\uparrow S\downarrow}{S\uparrow + S\downarrow} \tag{2.3}$$

where $S\uparrow$ is the uphill green speed, and $S\downarrow$ is the downhill green speed. Equation 2.3 reduces the error introduced by averaging green speeds in a green with elevation changes [9].

All of these perspectives on the putting behavior provide an important insight on the overall understanding of the sport. Ranging from purely experimental, empirical evidence, moving on to theoretical developments on the captured data, and finally to an entirely theoretical approach, these theories all have their validity, and their contributions to the understanding of the sport complement each other. The empirical models give us some good insight into what it is that

actually happens in a putt, and consider the influence of many aspects in the environment that can affect the outcome of each putt. The theoretical approach provides the perspective of a perfect putt. Using physics, some reasonable assumptions can lead to results that can imitate the behavior of a putt to an acceptable level of accuracy, which can lead to a model that can be readily used in practice by golfers of all knowledge levels.

A very powerful model can be developed by merging these two approaches. The theoretical model that predicts the putt to a marginally acceptable level of accuracy can be supplemented and fine-tuned by testing and considering the empirical models. Through experimentation, the parameters that more strongly influence the putting result (D_P) can be found, and can be given more scrutiny in the theoretical derivation in comparison to the rest of the parameters. Once a hybrid model is developed and corroborated through empirical means, its level of accuracy will be far superior to a standalone empirical or theoretical model.

The goal of the present study is to create hybrid model that is relevant and reliable to golfers in practice. The model will to describe the expected putting response from the most fundamental laws of physics, such as conservation of mass and momentum, and the laws of motion. These basic models will be strengthened by the empirical models obtained from research and experimentation. Finally, a hybrid theoretical and empirical model that predicts the two-dimensional displacement of the ball after impact based on the behavior of the putt as it is swung will be generated. This model will be applied in a straightforward manner for universal ease of use, while having the accuracy to be considered trustworthy and worthwhile for players and coaches in the sport.

Specifically, ratios of D_P to D_B will be developed for various putting conditions, to be used as rules of thumb in coaching.

CHAPTER 3: ANALYTICAL MODELING

Principles of classical mechanics were utilized in developing a model for the putting behavior. The putting motion was divided into three parts for analysis: (1) putter swing, (2) putter-ball collision, and (3) post-impact ball displacement. Two physics principles were employed to effectively describe the putting behavior: the principle of conservation of energy and the theory of impulse-momentum. The principle of conservation of energy was utilized to describe the pre-impact velocity of the putter as it is swung by the putter, as well as the post-impact displacement of the ball. Impulse-momentum theory was employed to describe the putter ball collision, in order to quantify the amount of energy imparted on the ball after impact from the putter.

In order to simplify the model for analysis, some assumptions were necessary (see Figure 3.1). The ball was analyzed as a rigid body, where energy is used for translational and rotational displacement. The dimples on the ball were considered to add a negligible effect to rotation and friction between the ball and the surface. The ball was also assumed to have negligible spin and bouncing after impact from the putter, or while being released from the stimpmeter. The cut of the grass of the green was assumed to be uniform, translating into a constant green speed and coefficient of friction throughout the surface. In analyzing the stroking motion, the putter was modeled as a pendulum, with a constant force input by the golfer, taken as the average force input through the stroke. The impact between the ball and the putter occurred at the point of the maximum velocity in the pendulum, which is more akin to the stroking motion of the novice golfers [2].

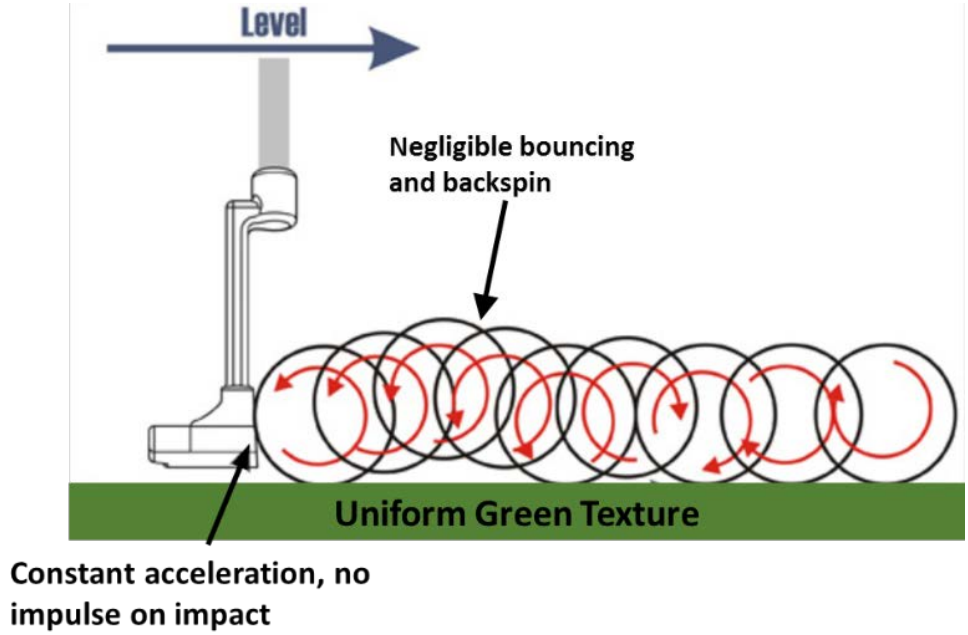

Figure 3.1 - Graphical Representation of the Assumptions in Putt Analysis

In the analysis of the pre-impact putter swing, the final velocity of the putter (V_{Pf}) is solely dependent on two factors, the initial height that the putter is brought and the work done by the golfer as the putter is swung. In order to simplify the analysis, a constant force input from the golfer was assumed. The constant force was considered the average of the force distribution throughout the swing. The equation derived for the final velocity of the putter was obtained from the law of conservation of energy:

$$E_0 = E_f \tag{3.1}$$

in the case of pre-impact putter swing, the initial energy, E_0, is simply the potential energy of the putter being held at a certain height (PE_P). The final energy, E_f, consists of the kinetic energy of

the putter, in addition to the work done by the golfer accelerating the putter (KE_f and W_P). Hence the equation can be rewritten as:

$$m_p gh + FR\beta = \frac{1}{2} m_p {v_{p_0}}^2 \tag{3.2}$$

where m_p is the mass of the putter, g is the acceleration due to gravity, h is the height at which the putter is brought, R is the combined length of the putter and golfer arm, β is half of the angle between the putter and the ball (see Figure 3.2), and v_{p_0} is the velocity of the putter at the end of the stroke. Manipulating this equation to describe the pre-impact velocity of the putter, v_{p_0}, as a function of all the other parameters, the resulting equation is

$$v_{p_0} = \sqrt{\frac{2(FR\beta + m_p gh)}{m_p}} \tag{3.3}$$

where all of the parameters are as described in Eq. 3.2.

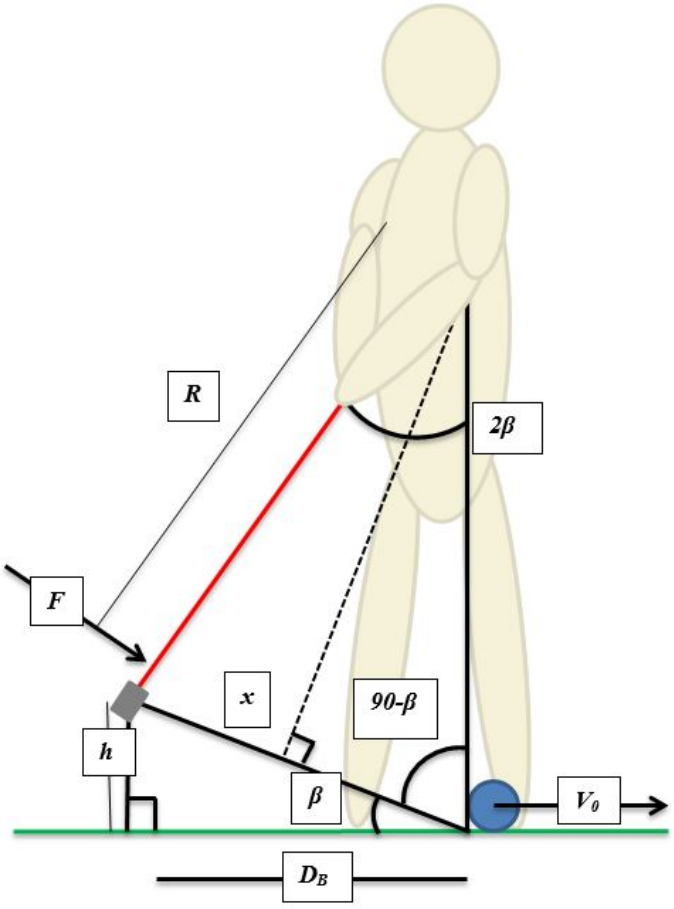

Figure 3.2 - Geometric Setup for the Analysis of Pre-impact Putter Swing

In order to simplify the model for golfers to readily employ in practice, some of the variables in Eq. 3.3 required modification. The initial height of the putter was reestablished as a function of D_B, and a relationship among half the angle between the putter and the vertical, β, and parameters that are more easily measured in the field was developed. An extensive analysis, based on Figure 3.2, of the geometry of the system yields the set of equations:

$$1 = \left(\frac{D_B}{2x}\right)^2 + \left(\frac{x}{R}\right)^2 \tag{3.4}$$

$$\cos(\beta) = \frac{D_B}{2x} \tag{3.5}$$

Where *2x* is the straight line distance from the ball to the putter head. Equations 3.4 and 3.5 can then be directly substituted into Equation 3.3 to provide a more practical prediction model for pre-impact putter velocity:

$$v_{p_0} = \sqrt{\frac{2\left(FR\beta + m_p gR\tan\beta\sin\beta\right)}{m_p}} \tag{3.6}$$

Based on these results, for a set of putts performed on a green, the only variables that control putter velocity are the average force imparted from the golfer, *F*, and the half angle between the putter and the vertical, β. The prediction model for pre-impact putter velocity demonstrates that a golfer can directly control the final speed of the putter by adjusting one or both of these parameters.

On the analysis of collision between the ball and the putter, the impulse-momentum theory of Physics was employed, as given by the equation

$$\Sigma\left(m_0 v_0\right)_i = \Sigma\left(m_f v_f\right)_i \tag{3.7}$$

where m_0 and m_f are the initial and final masses, and v_0 and v_f are the initial and final velocities, respectively. The product of the mass and velocity is called momentum. The momentum of every single body that is to be considered in a system is added on each side. In the case of this model, only the momentum of the ball and the putter needed to be included in the system. The pre-impact

velocity of the putter is obtained from the results of the putter swing analysis, Equation 3.6. The contact between the ball and the putter is assumed in a manner that negligible spin is introduced from the impact. During the impact, the impulse imparted by the golfer is also considered to be negligible. Taking into consideration these assumptions yields Equation 3.8 for the post-impact ball velocity:

$$v_{b_f} = \frac{(1+e)m_p v_{p_0}}{m_p + m_b} \tag{3.8}$$

where v_{b_f} is the final ball velocity, m_p and m_b are the putter and ball masses, respectively, e is the coefficient of restitution for the impact, and v_{p_0} is the initial putter velocity. Since the pre-impact putter velocity can be obtained by the model derived previously (Equation 3.6), it can be combined with the results for the post-impact ball velocity to obtain the following relationship:

$$v_{b_f} = \frac{(1+e)m_p}{m_p + m_b}\sqrt{\frac{2\left(FR\beta + m_p gR\tan\beta\sin\beta\right)}{m_p}} \tag{3.9}$$

This relationship can be used to predict the initial velocity of the golf ball after being impacted by the putter by considering the geometry of the putter swing, as well as the work done by the golfer accelerating the putter.

Lastly, the rolling of the ball after impact was modeled by reconsidering the conservation of energy principle of physics. The initial kinetic energy of the ball, which is imparted from the putter at impact, is dissipated by the friction between the ball and the turf as the ball rolls; however, in order to proceed with the analysis, it was necessary to establish a definition for the friction

between the ball and the turf that can be easily measured in a golf course, and that can be applicable to the majority of cases. The effectiveness of a green in impeding the rolling of the ball is dependent on several factors, such as the cut of grass, moisture on the turf, and irregularities in the terrain, and is variable by course. For golfers to have a better idea of what to expect when putting, golf courses generally provide a value for the speed of the green, sometimes also called stimp, which is a measure of how far a ball rolls after being released from a tool called a stimpmeter [7]. The speed of the green, D_g, is a value that many golf courses endeavor to provide with a fair degree of accuracy, and can thusly be related to the coefficient of friction in order to generate more accessible theoretical models.

In relating the speed of the green to the coefficient of friction, an energy analysis was carried out to describe how the energy is dissipated from rolling down the stimpmeter and on the turf. The stimpmeter has a notch where the ball is placed that allows it to be released at an angle, θ_g, of 20.5^o, on average. Using this knowledge, the energy loss of the ball as it rolls on a flat surface was calculated, yielding the following relationship the coefficient of friction of the green:

$$\mu_g = \frac{7}{10}\frac{V_g^2}{gD_g} \tag{3.10}$$

where μ_g is the coefficient of friction of the green, V_g is the velocity of the ball as it rolls off of the stimpmeter, g is the acceleration due to gravity, and D_g is the green speed.

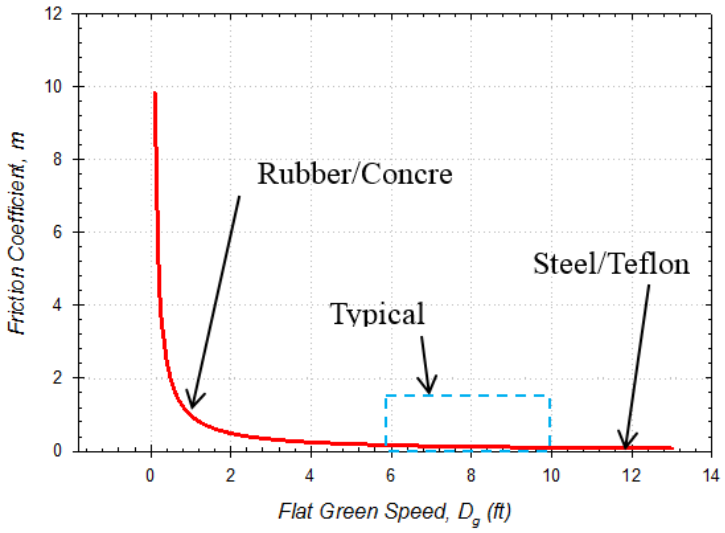

Figure 3.3 - Typical Friction Coefficient Ranges for Green Speed Measurements

From the derivation of Eq. 3.10, the coefficient of friction is inversely related to the speed of the green. Since the velocity with which the ball leaves the stimpmeter is a constant value of around 1.83 m/s [8], the speed of the green and the coefficient of friction can be considered to be solely dependent on each other on a flat surface. Figure 3 shows the coefficient of friction between the ball and the turf as a function of green speed. As demonstrated by the graph, green speeds can vary from 3.5 to 16+ feet, but are generally closer to 6 to 10 feet for most golf courses [10].

In the case of an incline in the green, described as an angle ϕ, an identical analysis was performed, with the exception of the consideration of the loss or gain of energy from the gravitational potential energy. Typical gradients on putting greens can go up to ±4%. The resulting relationship for coefficient of friction and speed of the green over a sloped green is

$$\mu = \frac{7}{10}\frac{V_0^2}{gD_g} - \tan(\phi) \tag{3.11}$$

where ϕ is the angle of inclination of the putting green. This is a generalized relationship for the coefficient of friction, μ, green speed, D_g, and slope of the green, ϕ. Note that in a slope of zero, Equation 3.11 reduces to Equation 3.10.

Once the relationship between the green speed and the coefficient of friction was established, an energy analysis could be performed for the rolling of the ball after impact. The analysis would follow the methods performed for calculating the coefficient of friction, but in this case, the unknown would be the travel distance of the ball. The equation obtained for the putt distance as a function of initial ball velocity and turf slope is

$$D_p = \frac{7}{10}\frac{V_0^2}{g\left(\frac{C_g}{D_g}\cos(\phi) + \sin(\phi)\right)} \tag{3.12}$$

where D_p is the putt distance, V_0 is the post-impact ball velocity, g is the acceleration due to gravity, C_g is the stimpmeter constant, as described by

$$C_g = L_g \cos\theta_g \sin\theta_g = 0.820 \tag{3.13}$$

where L_g is the length of the stimpmeter, around 91cm, D_g is the green speed, and ϕ is the angle of inclination of the green. Combining the equations that describe the swing (3.6), impact (3.8) and ball rolling (3.12) yield the equation

$$D_B = \frac{10}{7} C_c \left[\frac{m_b + m_p}{(1+e) m_p} \right]^2 \frac{g}{2a_P} \left(\frac{C_g}{D_g} \cos\phi + \sin\phi \right) D_P \tag{3.14}$$

where C_c is the impact correction factor, utilized to reduce error in practice, a_p is the average acceleration of the putter, related to the average force imparted on the putter by Newton's Second Law of Motion. Equation 3.14 shows that the putt distance is linearly related to backstroke. All of the other factors in this equation vary by putt or putting green, but the only variable that can be directly controlled by the golfer on a per putt basis is the backstroke. This implies that if a golfer desires a certain distance putt, the main factor to consider is the backstroke of the swing. Likewise, when predicting a putt distance, backstroke can be considered the most influential parameter.

Plugging in some common values, some trends can be found for the relationship between backstroke, putt distance and putter velocity, under different scenarios of green speed and elevation. Tables were developed for V_0 and D_B as a function of D_P, based on Eqs. 3.12 and 3.14 over different green speeds and elevations.

Table 3.1 - Table of Values for V_0 as a Function of D_P

V0 (m/s) with Green Speed of 2.44m (8ft)						
	1m	3m	5m	8m	10m	15m
0 degrees	2.17	3.76	4.85	6.14	6.86	8.41
10 degrees	2.66	4.61	5.95	7.52	8.41	10.30
20 degrees	3.04	5.26	6.79	8.59	9.60	11.76
30 degrees	3.33	5.77	7.45	9.42	10.53	12.90
45 degrees	3.64	6.30	8.14	10.29	11.51	14.09
V0 (m/s) with Green Speed of 2.44m (10ft)						
	1m	3m	5m	8m	10m	15m
0 degrees	1.94	3.36	4.34	5.49	6.14	7.52
10 degrees	2.48	4.29	5.54	7.01	7.84	9.60
20 degrees	2.89	5.00	6.46	8.17	9.13	11.18
30 degrees	3.20	5.55	7.17	9.06	10.13	12.41
45 degrees	3.55	6.14	7.93	10.03	11.21	13.73
V0 (m/s) with Green Speed of 2.44m (6ft)						
	1m	3m	5m	8m	10m	15m
0 degrees	2.51	4.34	5.60	7.09	7.92	9.71
10 degrees	2.94	5.08	6.56	8.30	9.28	11.37
20 degrees	3.27	5.66	7.31	9.25	10.34	12.67
30 degrees	3.53	6.11	7.89	9.98	11.16	13.66
45 degrees	3.79	6.56	8.47	10.71	11.98	14.67

Table 3.2 - Table of Values for D_B as a Function of D_P

Db (m) with Green Speed of 2.44m (10ft)						
	1m	3m	5m	8m	10m	15m
0 degrees	0.11	0.33	0.56	0.89	1.12	1.67
10 degrees	0.18	0.55	0.91	1.46	1.82	2.73
20 degrees	0.25	0.74	1.23	1.97	2.47	3.70
30 degrees	0.30	0.91	1.52	2.43	3.04	4.56
45 degrees	0.37	1.12	1.86	2.98	3.72	5.59
Db (m) with Green Speed of 2.44m (8ft)						
	1m	3m	5m	8m	10m	15m
0 degrees	0.14	0.42	0.70	1.12	1.39	2.09
10 degrees	0.21	0.63	1.05	1.68	2.09	3.14
20 degrees	0.27	0.82	1.37	2.18	2.73	4.10
30 degrees	0.33	0.98	1.64	2.63	3.28	4.92
45 degrees	0.39	1.18	1.96	3.14	3.92	5.88
Db (m) with Green Speed of 2.44m (6ft)						
	1m	3m	5m	8m	10m	15m
0 degrees	0.19	0.56	0.93	1.49	1.86	2.79
10 degrees	0.26	0.77	1.28	2.04	2.55	3.83
20 degrees	0.32	0.95	1.58	2.53	3.17	4.75
30 degrees	0.37	1.11	1.84	2.95	3.69	5.53
45 degrees	0.42	1.27	2.12	3.40	4.25	6.37

The ratio of D_B to D_P, which can be obtained from Eq. 3.14 and Table 3.5, clearly varies as the environmental parameters change, but a good rule of thumb that can be applied with acceptable accuracy, is that for every foot of backstroke, the putt distance will travel one foot less than the green speed on a flat surface. For example, at a green speed of 10ft, $\frac{D_B}{D_P}$ was found to be 8.96, an 8ft green speed yielded a ratio of 7.17, and 6 feet yielded a ratio of 5.38. Results from Eq. 3.14 can be found for all sorts of different scenarios, and rules of thumb can be developed for them in the same manner.

CHAPTER 4: EXPERIMENTAL APPROACH

Testing was performed to validate the theoretical models and provide a different perspective on the putting behavior. First, ball travel distance was measured for putts and green speed measurements. Measured D_P was compared to a predicted D_P based on the velocity of the ball, V_0 and the calculated theoretical coefficient of friction. Subsequently, D_P was predicted based on D_B by using Eq. 3.14. The experiments were performed on three turfs with different D_g: a course green (average speed), fairway (slow), and artificial turf (fast).

Testing on the artificial turf was performed using a SeeMore putter, Titleist ProV-1x golf balls, and an official USGA stimpmeter. The stroke was recorded by camera and data gathering was supplemented by the use of SAM PuttLab equipment. Error was calculated on each trial and a best fit was found for backstroke vs. putt distance.

Initial testing consisted on validating the derivation for the coefficient of friction as a function of the green speed. First, the green speed was measured with a stimpmeter. The improved green speed formula introduced by Brede [9] was utilized to reduce averaging error on the sloped surface. The average green speeds were 10.4, 3.85, and 11.6ft, with a slope of 1, 0, and 0^o for the green, fairway, and artificial turf, respectively, as measured with a protractor. Using the green speed, a coefficient of friction was calculated for each environment, and then utilized to predict a travel distance of the ball being released from the stimpmeter. Tables containing the data for testing the coefficient of friction relationship can be found in the Appendix (Tables 1, 2, and 3). The

average calculation error was 9% for the artificial turf, 22% for the fairway, and 32% for the green at 1% slope.

Once the data for the coefficient of friction was obtained, a second set of experiments was performed. Testing took place in the artificial turf location, and utilized the SAM PuttLab equipment to aid in recording the putts. In this trial the backstroke was recorded along with the putt distance in order to establish the empirical relationship between the two. A linear regression analysis was performed on the scatterplot of the data, which yielded Figure 4.1 and its empirical relationship:

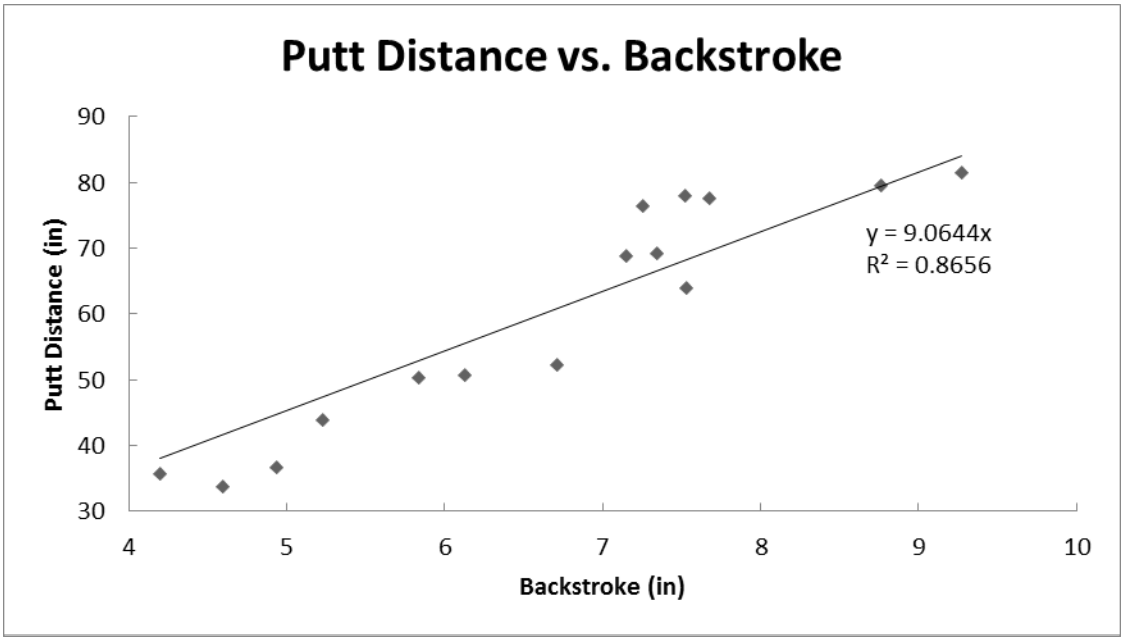

Figure 4.1 - Data for Putt Distance as a Function of Backstroke

As shown in the graph, the coefficient of determination is 0.866, suggesting a strong linear correlation and providing good preliminary support for the theoretical model of putt distance vs.

backstroke. The linear fit of D_P vs. D_B suggests a $\frac{D_P}{D_B}$ ratio of 9, which, for a green speed of 11.6 and a flat surface, underestimates the rule of thumb developed from Eq. 3.14 by 15%. Higher green speeds correlate to a more rapidly increasing $\frac{D_P}{D_B}$ ratio, and the empirical data demonstrate that the rule of thumb rapidly loses validity as D_g goes much over 10ft.

To supplement the testing, the SAM PuttLab database was accessed, and the putting profiles of the golfers in the Mike Bender Golf academy were obtained and analyzed. The acceleration and velocity profiles of the putting of golfers of all levels were compared. It was discovered that the acceleration profiles of most experienced golfers were superimposable. Figure 4.2 demonstrates a common acceleration and velocity profiles of five putts performed by an experienced golfer.

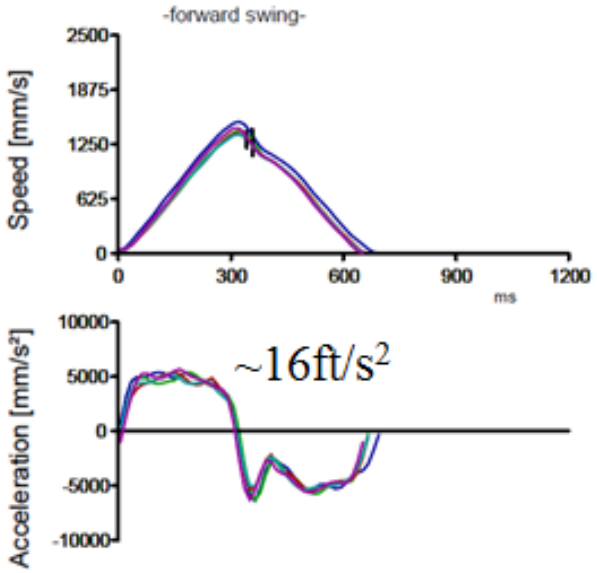

Figure 4.2 - Profile of Five Putts from an Experienced Golfer

It is shown in the graphs that the acceleration of the putt remains constant through the backstroke up until hitting the ball (around 350ms). Moreover, the putter acceleration over medium range putts is found to be around the same value of $16 ft/s^2$ for most of the experienced golfers with similar putting profiles. This fact helps validate the assumption of a constant force input from the golfer during the theoretical derivation of the putter velocity from the swing.

CHAPTER 5: NUMERICAL APPROACH

In light of the empirical results supporting corroborating the linear relationship between D_B and D_P, the next step is to unify the two theories, and expand on the developments that were initiated with the formulas. If the putt distance of the ball can be determined based on the backstroke of the putt in one dimension, the results can be expanded to two dimensions by applying the same rules. Furthermore, since the ball displacement calculations are dependent on Newton's Laws of Motion, results can be obtained with fair accuracy for any green with a uniform green speed and inclination.

These characteristics of the green, termed green texture, are not necessarily constant, however. In practice, it is more common to see a green with variable texture, with fluctuating elevations and varying green speeds. Since the laws of mechanics can approximate the behavior of the ball quite well for a constant acceleration, the more complex problem of varying texture can be simplified by dividing the process into many smaller, constant texture elements. The displacement and velocity for these elements can be calculated based on the laws of mechanics, and interlaced to describe the encompassing behavior of the ball. Taking this approach of finite elements allows the problem to be simplified to be within the realm of analyzability by the theory developed thus far, while maintaining a high degree of accuracy. The analysis of the post-impact behavior of the ball can be easily implemented by use of an algorithm that follows the laws of mechanics for every element.

The necessary input for the algorithm would be the surface texture, initial position, and the backstroke and direction of the putt. For the texture of the green, the topography can be

predetermined and stored in a database, or could be crudely scanned beforehand. The speed of the green can be obtained by use of the stimpmeter, but more than likely is provided by the facilities. The direction and backstroke of the green are the more variable of the input parameters of the algorithm, and as such, can be varied to provide useful, real time feedback to the golfer. From the direction and backstroke of the putt, the initial velocity of the ball can be determined. The acceleration of the ball will then be obtained from the texture of the green; the green speed will provide the friction force, and the slope of the green will provide the acceleration due to gravity. The green will be divided into many small elements, ranging from 100 to 4000 or more, as necessary (see Figure 5.1). From these parameters, the ball travel within each element can be calculated and plotted by utilizing Newton's Laws of Motion.

$$\begin{aligned} x_f &= x_0 + v_0 t + \frac{1}{2} a t^2 \\ v_f &= v_0 + at \\ {v_f}^2 &= {v_0}^2 + 2a\Delta x \end{aligned} \tag{5.1}$$

The ending position and velocity of the ball, as calculated by the set of equations in 5.1, will be the initial conditions of the next element, and the process will be repeated until the ball stops, or rolls out of bounds.

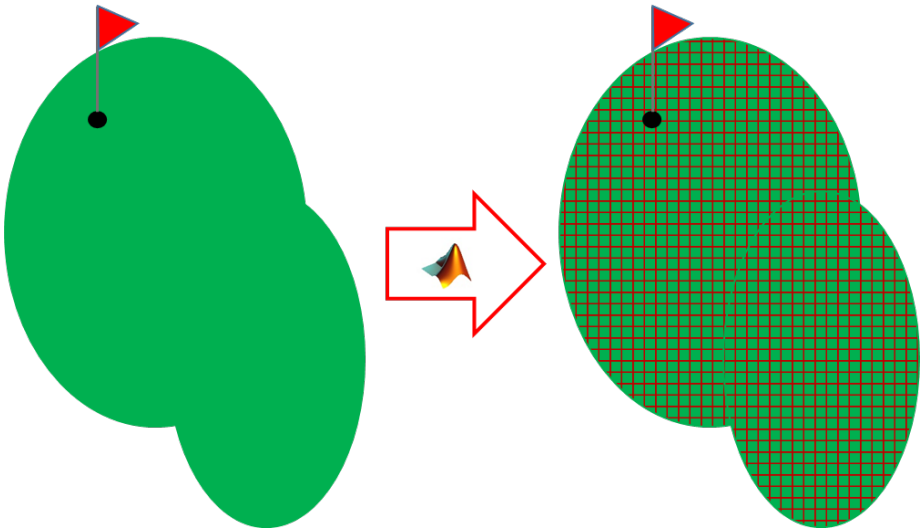

Figure 5.1 - Illustration of the Element Overlay on a Putting Green

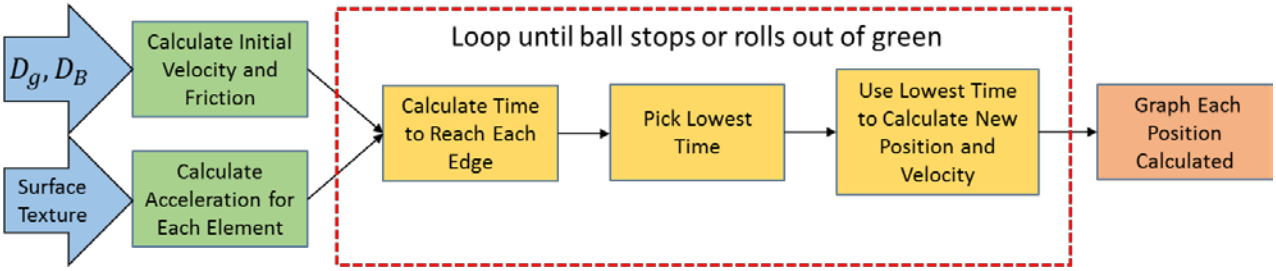

Figure 5.2 - Flow Chart of the Putt Prediction Algorithm

After iterating over the necessary number of elements, whether the ball completely stops or travels out of bounds, the algorithm stops, and the plotted positions will display the total displacement of the ball (see Figure 5.2). An x-y plot will provide a top down view of the ball travel on the green, enabling the golfer to see the predicted path of the ball, and make corrections as necessary. The program will perform a two dimensional analysis of the path of the ball, based on D_B, by using Eq. 3.14 followed by iterating equations 5.1 over each element.

CHAPTER 6: ALGORITHM RESULTS

The algorithm was tested for many different scenarios. Green size, ball speed (V_0) and initial location (x_0, y_0), green speed (D_g), and elevation (ϕ) were the variables that were modified to simulate several different scenarios. For each of the possible cases that can be constructed by combining different values of these variables, the number of elements was also varied. As can be inferred from the number of variables and the possible combination, there are vast amounts of scenarios that need to be considered in order to design a robust algorithm.

For the sake of testing, green size varied from 10m to 100m, ball speed in both directions varied from 0m/s to 100m/s, with directional angles (x-position/y-position) varying from 0^o to 90^o, initial location varied from 0% to 100% of the green length in both dimensions, green speed varied from 1ft to 16ft (measured in feet for ease of use in practice, but converted to meters in the algorithm), and the elevation varying from 0% to 100% grade incline (0^o to 45^o slope). As evidenced by the values attained by the variables, the test cases can become extreme for some combinations, and were only considered for testing the extent to which the stability of the algorithm can be taken. Despite the esoteric scenarios, the developed program was able to execute the algorithm and display results that were meaningful and reasonable for the given data. For several of the more reasonable scenarios, the results of each step were gathered and compared to calculations performed by hand. For up to 400 elements (a 20x20 element matrix for a green), only uncertainty present in the calculations was due to rounding errors in floating point operations.

The testing phase of the program began by maintaining a constant, average green speed of 8ft which is described by Weber as a medium, and thus reasonable, speed for a green [10]. The elevation for the first few trials was maintained at zero, in order to isolate the effects of friction on the acceleration. The green length was established to be 10m, and a 10x10 element matrix was utilized for a total of 100 elements with dimensions of 1m by 1m. The dimensions of the elements and the green were selected as such in order to be easily computable by hand, since the first few results were to be compared to manual calculations for consistency. The first test cases were executed with an initial velocity of magnitudes varying from 1 to 15m/s and directions from 15 to 75^o in 15^o intervals.

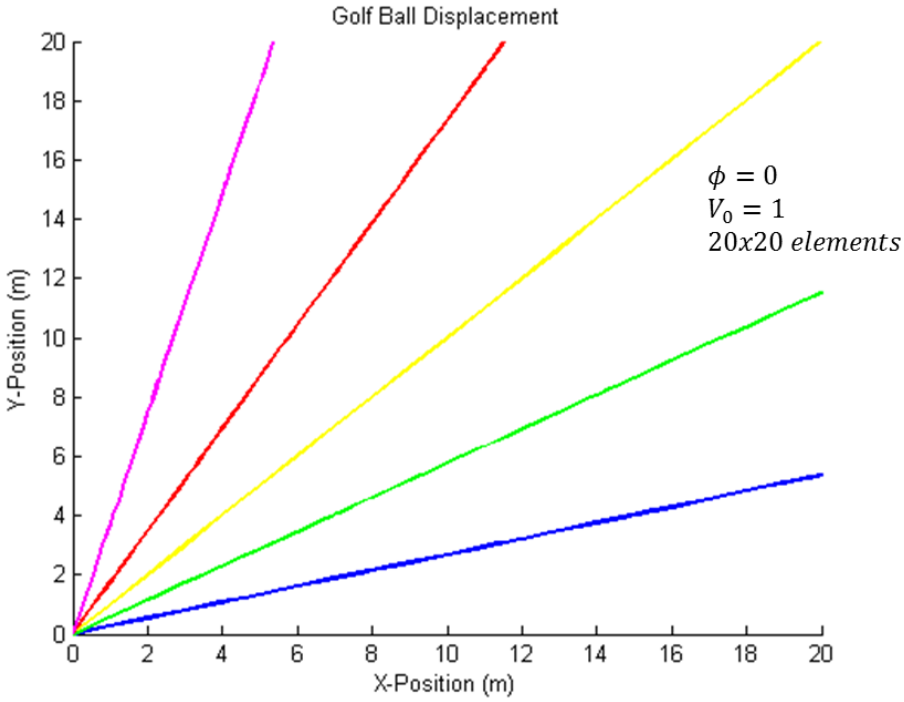

Figure 6.1 - Initial Velocity Test Cases

The results from initial velocity testing are as expected. From an initial position of 0m on both dimensions, and with enough speed imparted on the ball to ensure no stopping, the ball will travel a straight path at the angle in which it was released. The final position of the ball, as calculated by MATLAB, was compared to calculations performed by hand, in order to gauge the uncertainty introduced by rounding errors over several iterations. Table 6.1 illustrates the results of the error analysis on the algorithm.

Table 6.1 - Error Analysis for Algorithm vs. Hand Calculations

Test	X-Position			Y-Position		
	Algorithm	Theoretical	Error	Algorithm	Theoretical	Error
0 degrees	20	20	0	10	10	0
15 degrees	20	20	0	5.3578	5.1764	0.035044
30 degrees	20	20	0	11.5443	10	0.15443
45 degrees	20	20	0	19.9941	20	0.000295
60 degrees	11.5524	10	0.15524	20	20	0
75 degrees	5.3642	5.1764	0.03628	20	20	0
90 degrees	10.003	10	0.0003	20	20	0

The error was found to be a maximum of 15.5% in the case of 30 and 60^o from the horizontal. This error is introduced by rounding every time the ball reaches a new quadrant, and is more pronounced at those angles. While approaching 0 or 90^o, the error reduces to zero.

After obtaining acceptable results for the initial case, the velocity magnitude and direction were modified to test for consistency among different combinations. With green speed, size, and elevation remaining unchanged, the initial velocity was adjusted for values ranging from 0.5m/s to 20m/s of magnitude, and directed between 0^o and 90^o from the x-axis. The varied combination of magnitudes and directions were selected to cover the span of nonzero velocity

cases with zero elevation. All of these cases were calculated with a 10x10 or 20x20 element matrix, as previously described. Figure 6.2 illustrates how the change in initial direction relates to the ball displacement.

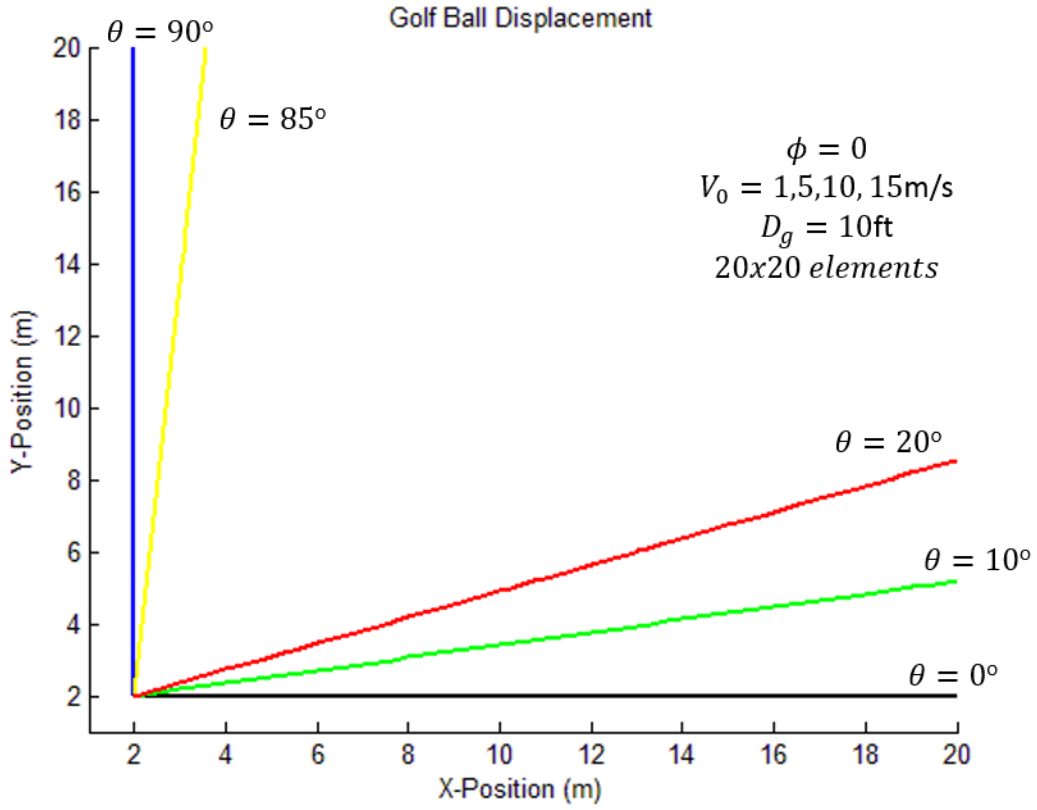

Figure 6.2 - Initial Velocity Testing over Varied Angles and Magnitudes

The presence of uncertainty in the algorithm calculations, and its invariance with respect to the initial velocity of the ball suggest an interesting concept. It would be of benefit to find the uncertainty of the calculations in relation to the number of iterations in the algorithm. With an understanding of said relationship, an upper bound for the number of elements can be established for a desired level of accuracy. With the goal of determining the maximum number of iterations

before the algorithm incurs a significant amount of uncertainty, a basic test case was developed, in which the number of elements in the matrix mapping the green were varied, while the other parameters remained constant. For a velocity of magnitude of 1m/s, no elevation, and a green speed of 8ft, spanning over a 10m square green, the matrix size was modified from 100x100 to 2000x2000. Figure 6.3 demonstrates the effects of increasing number iterations on calculation error.

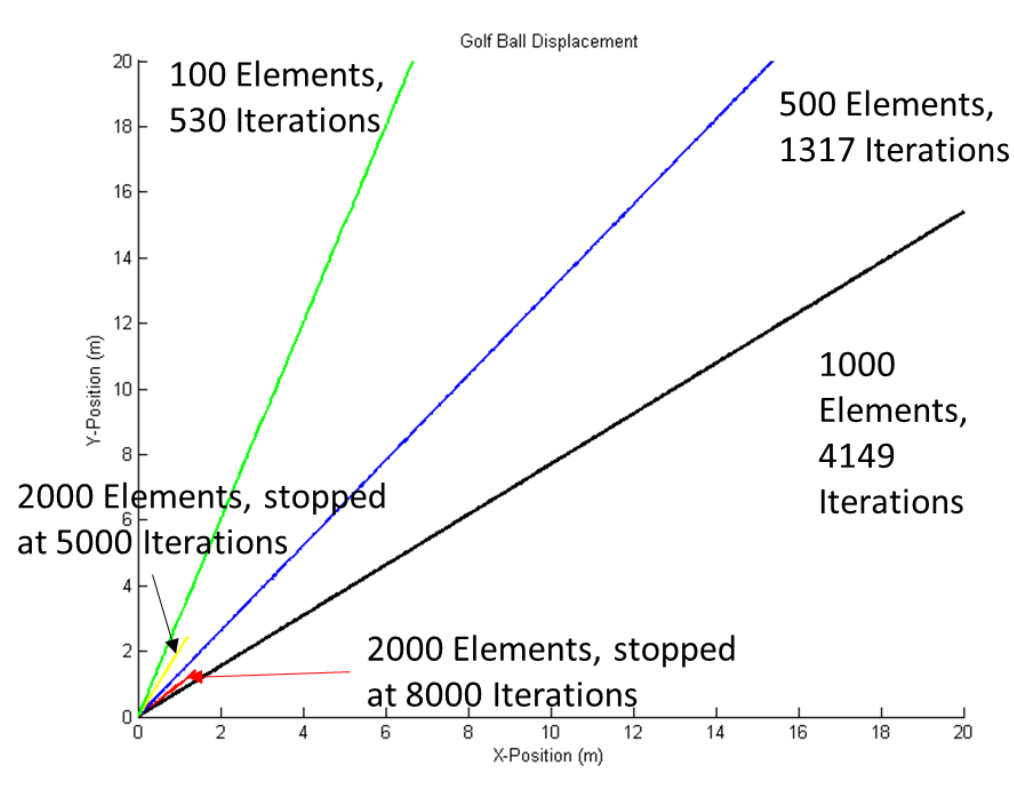

Figure 6.3 - Effects of Element Matrix Size on Predicted Ball Path

The results of these test cases show how the uncertainty compounds with increasing iteration size, to the point of the program not being able to continue the calculations with

reasonable efficiency. As the number of elements increase, the number of iterations increase much more, while demonstrating no significant advantage to accuracy. In order to perform the calculations efficiently, the optimum number of elements is 20x20. Anywhere between 10x10 and 50x50 produce the desired results without an excessive amount of calculations

The next few test cases involved testing a velocity in one direction only, as well as introducing a constant increase in elevation. In the case of zero elevation change, a purely one dimensional velocity yielded expected results, with no significant uncertainty in the calculations. Introducing a constant elevation change for the given test cases supported the theoretical calculations as well, with Figure 6.4 demonstrating the effects of a slight inclination accelerating a ball with initial velocity in one dimension only.

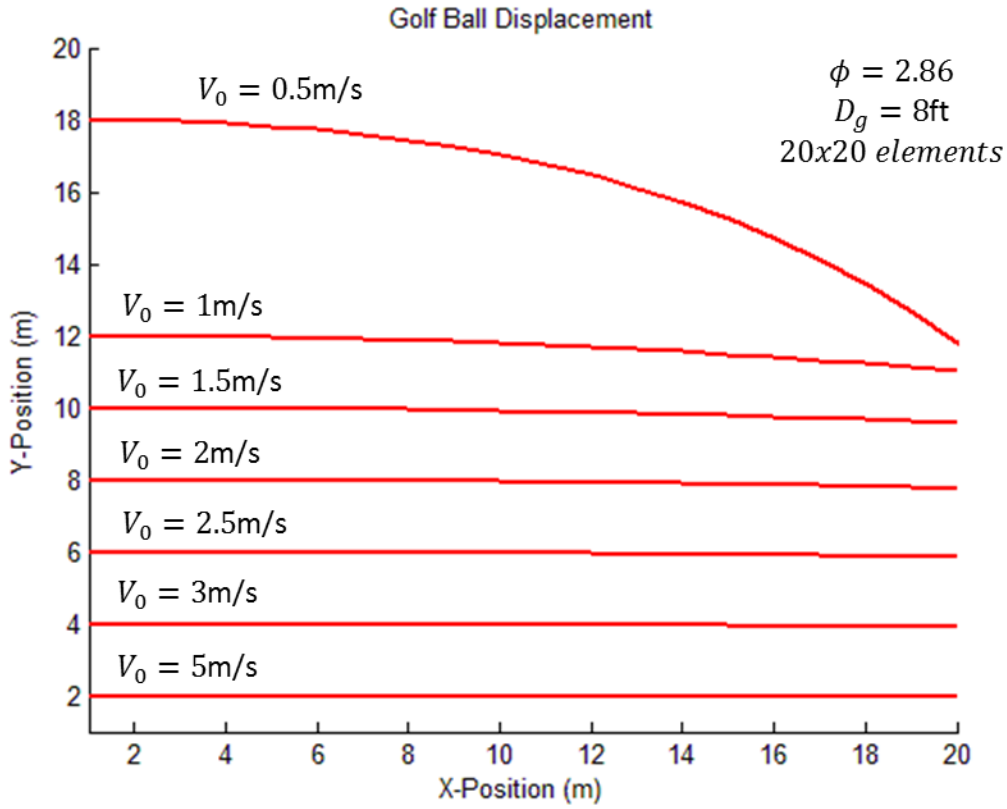

Figure 6.4 - One Dimensional Velocity Profile with Constant Slope

As expected, the ball moves slightly downward as the elevation increases with increasing position. With the constant elevation not introducing any demonstrable issues with the output in the algorithm, the complexity of the test cases was increased. A constantly increasing elevation was introduced into the cases, and Figure 6.5 demonstrates the effects on the ball displacement.

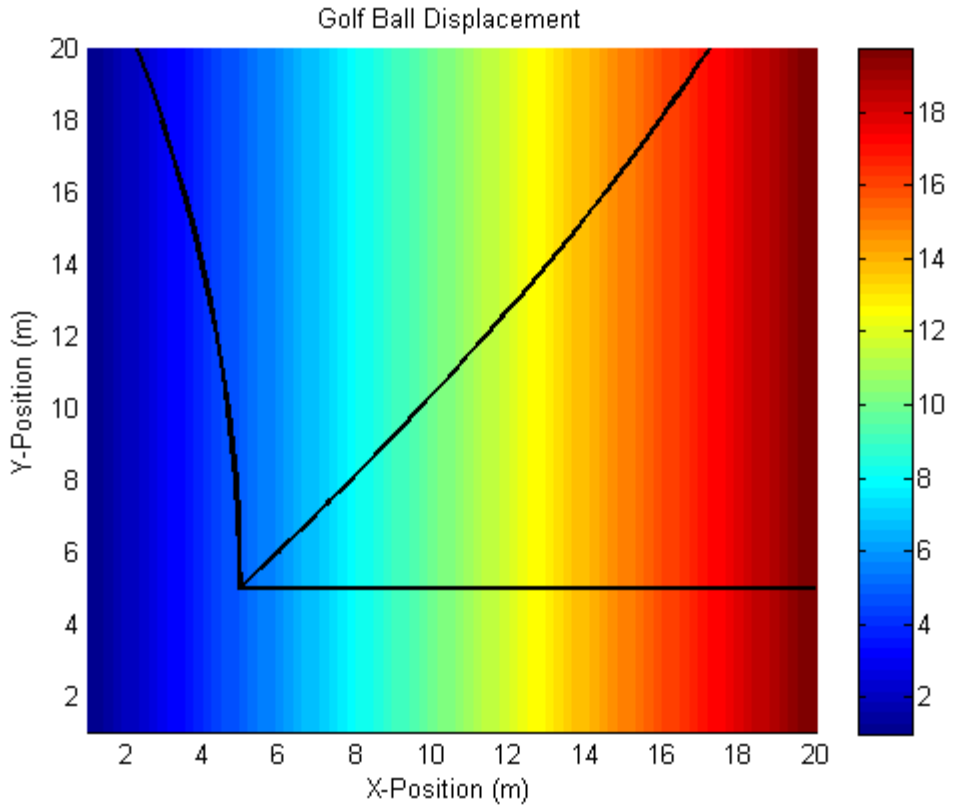

The elevation in these figures is illustrated by the background color of the graph, with blue being the lowest elevation (0m), and red representing the highest elevation (20m). As can be evidenced from the figure, the ball displacement displayed by the algorithm agrees with the established theory. In the case of vertical velocity only, the ball traveling in a horizontally increasing elevation will have its direction change over every iteration. Furthermore, if the ball travels in the direction of the elevation increase, the ball velocity will only change in magnitude, and not direction. Finally, a two dimensional velocity with a gradient changing in one dimension only was tested for the algorithm, and the calculations were performed as expected, combining the horizontal change in displacement with the two dimensional translation.

After a comprehensive testing battery, the program showed robustness to a varied combination of scenarios, ranging from the expected combinations found in practice, to more exotic cases that are less probable, all the way to extreme scenarios that push the boundaries of the algorithm. Furthermore, the algorithm executed the calculations with minimal uncertainty, ranging from 0% to a maximum of 15.5% under unlikely scenarios. In practice, the algorithm can be expected to work under the vast majority of scenarios with an average error under 15%, as evidenced by test cases that emulate the most probable scenarios.

CHAPTER 7: RULES OF THUMB FOR GOLFERS AND COACHES

Now that a theoretical model for putting has been developed and enhanced into a putt distance prediction model, much can be done with the results obtained from each model in conjunction with the experimental results. Starting off with the backstroke model, Equation 3.14 can be modified to provide the ratio of $\frac{D_P}{D_B}$

$$\frac{D_P}{D_B} = \left[\frac{10}{7} C_c \left[\frac{m_b + m_p}{(1+e)m_p} \right]^2 \frac{g}{2a_P} \left(\frac{C_g}{D_g} \cos\phi + \sin\phi \right) \right]^{-1} \tag{7.1}$$

The two influencing factors in this ratio are now D_g and ϕ, the texture of the green. As these two parameters are varied, a relationship can be found between the parameters, and the $\frac{D_P}{D_B}$ ratio. Table 7.1 illustrates the values that were obtained for a variation of angles and green speeds.

Table 7.1 - $\frac{D_P}{D_B}$ Ratio Over Different ϕ and D_g Values

DP/Db		Dg (ft)										
		5	**6**	**7**	**8**	**9**	**10**	**11**	**12**	**13**	**14**	**15**
Angle (degrees)	**0**	4.5	5.4	6.3	7.2	8.1	9.0	9.9	10.7	11.6	12.5	13.4
	5	3.9	4.5	5.1	5.7	6.3	6.8	7.3	7.8	8.2	8.6	9.1
	10	3.4	3.9	4.4	4.8	5.1	5.5	5.8	6.1	6.4	6.6	6.9
	15	3.1	3.5	3.8	4.1	4.4	4.6	4.9	5.1	5.3	5.4	5.6
	20	2.8	3.2	3.4	3.7	3.9	4.1	4.2	4.4	4.5	4.6	4.7
	25	2.6	2.9	3.1	3.3	3.5	3.6	3.7	3.9	3.9	4.0	4.1
	30	2.5	2.7	2.9	3.0	3.2	3.3	3.4	3.5	3.5	3.6	3.7
	35	2.4	2.6	2.7	2.8	2.9	3.0	3.1	3.2	3.2	3.3	3.3
	40	2.3	2.4	2.6	2.7	2.8	2.8	2.9	3.0	3.0	3.0	3.1
	45	2.2	2.4	2.5	2.5	2.6	2.7	2.7	2.8	2.8	2.9	2.9

The $\frac{D_P}{D_B}$ ratio clearly increases with increasing D_g, and decreases with increasing ϕ. The data for Table 7.1 were plotted to provide a more visual representation of the trends.

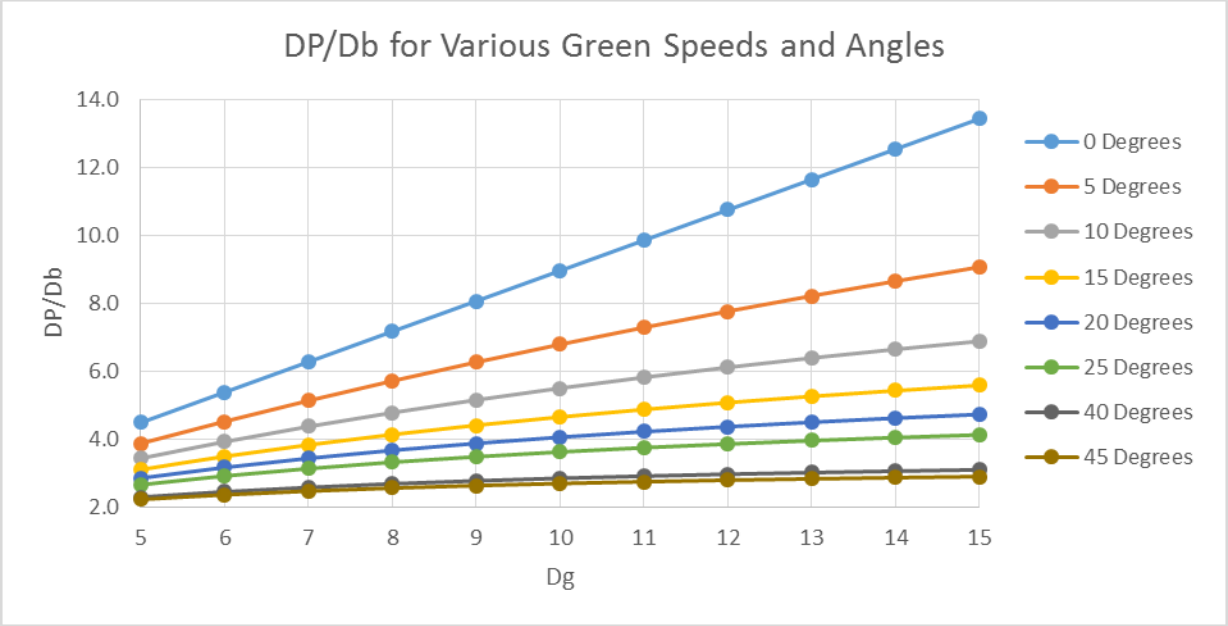

Figure 7.1 - Trends in $\frac{D_P}{D_B}$ Ratio

The data graphs illustrate the increasing ratio with increasing D_g, but also demonstrate a slower rate of change for higher ϕ. As a rule of thumb, however, it can be safely assumed that for an average green speed of 10ft and a flat surface, the $\frac{D_P}{D_B}$ ratio is 9 to 1. For every foot of backstroke, the putt should travel 9 feet. Any increase or decrease in green speed from this point can be translated into an equal increase or decrease in $\frac{D_P}{D_B}$ ratio. These numbers agree with the experimental findings, which for a green speed of 11.6ft on the artificial turf, the experimental $\frac{D_P}{D_B}$ ratio was

found to be 9.1, close to the calculated value of 9.9. For every angle increase in ϕ, the $\frac{D_P}{D_B}$ ratio can be decreased by 0.5.

CHAPTER 8: CONCLUSIONS AND FUTURE WORK

By utilizing the principles of classical mechanics, a theoretical model that describes the behavior of putting and the post-impact displacement of the ball was developed. The resulting model identified the post impact putt distance to be directly proportional to the backstroke of the putt. Field testing of putting and ball travel yielded results that corroborated the theoretical findings. Furthermore, the empirical models demonstrated a linear correlation between backstroke length and putt distance, with the constant of proportionality factoring in all of the outside parameters (see Equation 3.14). Testing of the developed formula shows promising preliminary results for the backstroke equation. The first trial of testing (91 samples), which only considered ball rolling and friction yielded an error as low as 9% for high speed greens (speed of ~12 feet), and as high as 32% for the lowest speed turfs (~6 feet). When predicting putt distance based on backstroke, by implementing the formula for the given data, the error averaged 5% over 15 samples.

With an acceptable prediction consistency, as proven by the experimental developments, the backstroke formula was expanded to predict the ball displacement in two dimensions by being implemented into a finite element analysis algorithm. This algorithm takes in the initial backstroke and direction of a putt, calculates the initial ball velocity through Equation 3.14, and predicts the path of the ball through an iterative process. Comprehensive testing of the implemented algorithm demonstrate remarkable robustness for varied conditions, while maintaining a reliable degree of accuracy. Testing of more than 100 different combinations of values yield very accurate qualitative

results. In depth testing of the putt distance predictive algorithm yield results that are within less than 10% of theoretical values.

The high degree of reliability, combined with the preciseness of the putt distance prediction model demonstrate remarkable promise for its success in practice. With the only necessary inputs being the backstroke and direction of the putt, this model provides dependable feedback to the putter with minimal effort and high reliability. The simplicity of the algorithm also allows it to be implemented in real time, providing a quick rendering of the ball displacement as the putter is moved or the input is changed by manually. For a golfer, being able to accurately visualize the path of the ball for a given putt without having to move the putter can prove to be a remarkable aid, and the findings developed in analyzing the post-impact ball displacement bring this goal one step closer to being feasible.

APPENDIX A:

DATA TABLES

Table A.1 - Data Gathered for Friction vs. Green Speed Comparison on Artificial Turf

Artificial Turf					
Distance Dp (in)	Time (s)	Initial Velocity V0 (ft/s)	Coefficient of Friction μ	Calculated Distance Dp (in)	Error
68.8	0.15	4.17	0.066	60.4	0.122
66.7	0.15	4.17	0.068	60.4	0.094
64.4	0.15	4.17	0.070	60.4	0.062
68.6	0.133	4.70	0.084	76.9	0.121
68.6	0.134	4.66	0.083	75.7	0.104
65.4	0.15	4.17	0.069	60.4	0.076
73.1	0.134	4.66	0.078	75.7	0.036
62.9	0.15	4.17	0.072	60.4	0.039
63.7	0.133	4.70	0.090	76.9	0.207
63.7	0.15	4.17	0.071	60.4	0.051
68.4	0.134	4.66	0.083	75.7	0.107
75.8	0.133	4.70	0.076	76.9	0.014
59	0.15	4.17	0.077	60.4	0.024
65.4	0.15	4.17	0.069	60.4	0.076
74.4	0.133	4.70	0.077	76.9	0.033
69.3	0.15	4.17	0.065	60.4	0.128
74.6	0.134	4.66	0.076	75.7	0.015
82	0.133	4.70	0.070	76.9	0.062
81.2	0.134	4.66	0.070	75.7	0.067
72	0.133	4.70	0.080	76.9	0.068
74.1	0.15	4.17	0.061	60.4	0.184
82.1	0.133	4.70	0.070	76.9	0.064
75.5	0.15	4.17	0.060	60.4	0.199
85	0.133	4.70	0.068	76.9	0.096
91	0.117	5.34	0.082	99.3	0.092
85.4	0.133	4.70	0.067	76.9	0.100
84.5	0.134	4.66	0.067	75.7	0.104
79.4	0.15	4.17	0.057	60.4	0.239
76.8	0.133	4.70	0.075	76.9	0.001
83.2	0.134	4.66	0.068	75.7	0.090
Average		4.50	0.072	70.5	0.089

Table A.2 - Data Gathered for Friction vs. Green Speed Comparison on Fairway

Fairway					
Distance Dp (in)	Time (s)	Initial Velocity V0 (ft/s)	Coefficient of Friction μ	Calculated Distance Dp (in)	Error
28.7	0.183	3.64	0.121	17.1	0.403
29.6	0.183	3.64	0.117	17.1	0.421
34.8	0.15	4.44	0.148	25.5	0.267
31.5	0.183	3.64	0.110	17.1	0.456
35.9	0.15	4.44	0.144	25.5	0.289
30.6	0.183	3.64	0.113	17.1	0.440
33.4	0.15	4.44	0.154	25.5	0.236
35.9	0.15	4.44	0.144	25.5	0.289
39.2	0.133	5.01	0.167	32.5	0.172
35.9	0.15	4.44	0.144	25.5	0.289
37.2	0.134	4.98	0.174	32.0	0.141
33.9	0.167	3.99	0.123	20.6	0.393
38.1	0.167	3.99	0.109	20.6	0.460
36	0.15	4.44	0.143	25.5	0.291
28.6	0.134	4.98	0.226	32.0	0.118
30.4	0.15	4.44	0.170	25.5	0.161
27.9	0.133	5.01	0.235	32.5	0.163
31	0.133	5.01	0.211	32.5	0.047
35.7	0.117	5.70	0.237	41.9	0.175
31.8	0.133	5.01	0.206	32.5	0.021
35	0.117	5.70	0.242	41.9	0.198
32.8	0.133	5.01	0.200	32.5	0.010
35.9	0.116	5.75	0.240	42.7	0.188
36	0.117	5.70	0.235	41.9	0.165
31.8	0.133	5.01	0.206	32.5	0.021
40.2	0.116	5.75	0.214	42.7	0.061
34.9	0.134	4.98	0.185	32.0	0.084
35.5	0.117	5.70	0.239	41.9	0.181
Average		4.75	0.177	29.1	0.219

Table A.3 - Data Gathered for Friction vs. Green Speed Comparison on Green

Green					
Distance Dp (in)	Time (s)	Initial Velocity V0 (ft/s)	Coefficient of Friction μ	Calculated Distance Dp (in)	Error
76	0.1	6.25	0.117	88.3	0.162
74.8	0.1	6.25	0.119	88.3	0.181
67.2	0.116	5.39	0.095	65.6	0.023
67.1	0.1	6.25	0.134	88.3	0.316
75.5	0.101	6.19	0.115	86.6	0.147
77.1	0.1	6.25	0.115	88.3	0.145
73.8	0.1	6.25	0.121	88.3	0.197
77.3	0.1	6.25	0.114	88.3	0.142
76.3	0.116	5.39	0.082	65.6	0.140
111.2	0.067	9.33	0.187	196.7	0.769
106.8	0.083	7.53	0.121	128.2	0.200
108.4	0.083	7.53	0.119	128.2	0.183
40.3	0.15	4.17	0.095	39.3	0.026
41.4	0.167	3.74	0.071	31.7	0.235
39.9	0.183	3.42	0.059	37.8	0.052
103.3	0.133	4.70	0.038	71.6	0.307
98.4	0.133	4.70	0.041	71.6	0.273
99.1	0.133	4.70	0.041	71.6	0.278
113.6	0.117	5.34	0.048	92.5	0.186
121.6	0.134	4.66	0.029	70.5	0.420
123.1	0.117	5.34	0.043	92.5	0.249
90	0.15	4.17	0.033	56.3	0.375
110.5	0.134	4.66	0.034	70.5	0.362
105.4	0.15	4.17	0.026	56.3	0.466
105.4	0.177	3.53	0.013	40.4	0.617
111.9	0.133	4.70	0.034	71.6	0.360
107.8	0.177	3.53	0.013	40.4	0.625
56.2	0.233	2.68	0.016	23.3	0.585
64.5	0.217	2.88	0.016	26.9	0.583
69	0.184	3.40	0.026	37.4	0.458
64	0.233	2.68	0.012	23.3	0.636
60.7	0.217	2.88	0.018	26.9	0.557
Average		4.966	0.067	79.9	0.320

Table A.4 - D_B vs. D_P Table of Data

Artificial Turf						
Backstroke Length (in)	Putt Distance Dp (in)	Velocity of Putter Vp0 (ft/s)	Velocity of Ball V0 (ft/s)	β (rad)	Theoretical Ball Velocity V0 (ft/s	Theoretical Distance Dp (in)
7.53	64.0	3.28	6.50	0.08	6.37	70.7
7.34	69.3	3.30	6.54	0.08	6.28	68.7
9.27	81.5	3.67	7.27	0.10	7.19	90.1
8.76	79.5	3.46	6.86	0.10	6.96	84.3
7.68	77.5	3.46	6.86	0.08	6.44	72.3
7.25	76.5	3.42	6.77	0.08	6.24	67.7
7.15	68.8	3.19	6.33	0.08	6.19	66.6
7.52	78.0	3.50	6.93	0.08	6.37	70.6
4.93	36.8	2.57	5.09	0.05	5.02	43.9
4.20	35.8	2.42	4.79	0.05	4.60	36.8
4.60	33.8	2.33	4.62	0.05	4.83	40.7
5.23	44.0	2.63	5.22	0.06	5.19	46.9
6.71	52.3	2.90	5.74	0.07	5.97	62.0
6.13	50.8	2.79	5.54	0.07	5.67	55.9
5.84	50.3	2.70	5.35	0.06	5.52	53.0

APPENDIX B:

ALGORITHM CODE

```
%Pascual Santiago-Martinez
%Putt Distance Calculator Version 2.0
%Calculates the ball trajectory after impact from the putter

%Input the dimensions of the green
XGreenLen = 20;
YGreenLen = 20;

%Known parameters
%GreenSpeed multiple is to convert to meters
%Count will be used for graphing
GreenSpeed = 8 * 0.3048;
XPos = 1;
YPos = 18;
count = 1;

%Calculate initial velocity from backstroke equation
VXIni = .45*cos(00*3.141/180);
VYIni = 1*sin(00*3.141/180);

%Load the green texture from a .txt file.
%Data is expected to be in square matrix form
XGreenSlope = load('XGreenSlope.txt');
YGreenSlope = load('YGreenSlope.txt');
[YNumElements, XNumElements] = size(XGreenSlope);

%Calculate the acceleration of the ball of each element based on
%known parameters
%Coefficient of friction and acceleration in x and y directions based on
%slopes
XFric = -(0.7 * 1.83 ^ 2 / 9.8 / GreenSpeed) * 9.8 * 0.01 * cos(atan(XGreenSlope));
XAccel = -9.8 * 0.01 * sin(atan(XGreenSlope));

YFric = -(0.7 * 1.83 ^ 2 / 9.8 / GreenSpeed) * 9.8 * 0.01 * cos(atan(YGreenSlope));
YAccel = -9.8 * 0.01 * sin(atan(YGreenSlope));

%Calculate the length and width of each grid
XGridLen = XGreenLen / XNumElements;
YGridLen = YGreenLen / YNumElements;

%Calculate the current quadrant of the ball
QuadX = floor(XPos / XGridLen) + 1;
QuadY = floor(YPos / YGridLen) + 1;
```

Code Screenshot 1

```
%initialize the graphing matrix
GraphX = zeros(1,1);
GraphY = zeros(1,1);
Color = zeros(1,1);

%add current position to graph array
GraphX(count) = XPos;
GraphY(count) = YPos;
color(count) = sqrt(VXIni^2 + VYIni^2);

%The algorithm will keep updating the position of the ball as long as the
%ball is not completely stopped and is within the designated surface
while ((VXIni ~= 0 || VYIni ~= 0) && (QuadX <= XNumElements && ...
        QuadY <= YNumElements) && (QuadX > 0 && QuadY > 0))

    t = -1;
    %Get the time the ball takes to reach next quadrant (if at all) in x
    if(4 * VXIni ^ 2 + 8 * XAccel(YNumElements-QuadY+1,XNumElements-QuadX+1) * (QuadX * XGridLen - XPos) > 0)
    TX = (-2 * VXIni + sqrt(4 * VXIni ^ 2 + 8 * (sign(VXIni) * XFric(YNumElements-QuadY+1,XNumElements-QuadX+1) +...
         XAccel(YNumElements-QuadY+1,XNumElements-QuadX+1)) *(QuadX * XGridLen - XPos))) / (2 * ...
         (sign(VXIni) * XFric(YNumElements-QuadY+1,XNumElements-QuadX+1) +...
         XAccel(YNumElements-QuadY+1,XNumElements-QuadX+1)));
    end

    if(XAccel == zeros(YNumElements, XNumElements))
        TX = (QuadX * XGridLen - XPos)/VXIni;
    end

    %if the ball reaches the next quadrant in the x direction, this will
    %be the time used for the distance calculation
    if(TX > 0)
        t = TX;
    end

    %Get the time the ball takes to reach next quadrant (if at all) in y
    if(4 * VYIni ^ 2 + 8 * YAccel(YNumElements-QuadY+1, XNumElements-QuadX+1) * (QuadY * YGridLen - YPos) > 0)
    TY = (-2 * VYIni + sqrt(4 * VYIni ^ 2 + 8 * (sign(VYIni) * YFric(YNumElements-QuadY+1,XNumElements-QuadX+1) +...
         YAccel(YNumElements-QuadY+1,XNumElements-QuadX+1)) *(QuadY * YGridLen - YPos))) / (2 * ...
         (sign(VYIni) * YFric(YNumElements-QuadY+1,XNumElements-QuadX+1) +...
         YAccel(YNumElements-QuadY+1,XNumElements-QuadX+1)));
    end
```

Code Screenshot 2

```
if(YAccel == zeros(YNumElements, XNumElements))
    TY = (QuadY * YGridLen - YPos)/VYIni;
end


%if the ball reaches the nex quadrant in the y direction before the x
%direction, update the t variable to use later
if(TY > 0 && TY < TX || t == -1)
    t = TY;
end


%Get the time the ball takes to reach previous quadrant (if at all) in x
if(4 * VXIni ^ 2 + 8 * XAccel(YNumElements-QuadY+1,XNumElements-QuadX+1) * ((QuadX - 1) * XGridLen - XPos) > 0 && VXIni < 0)
TX = (-2 * VXIni + sqrt(4 * VXIni ^ 2 + 8 * (sign(VXIni) * XFric(YNumElements-QuadY+1,XNumElements-QuadX+1) +...
     XAccel(YNumElements-QuadY+1,XNumElements-QuadX+1)) *((QuadX-1) * XGridLen - XPos))) / (2 * ...
     (sign(VXIni) * XFric(YNumElements-QuadY+1,XNumElements-QuadX+1) +...
     XAccel(YNumElements-QuadY+1,XNumElements-QuadX+1)));
end

if(XAccel == zeros(YNumElements, XNumElements))
    TX = abs(((QuadX - 1) * XGridLen - XPos)/VXIni);
end

%Update the time for calculations if it is smaller
if((TX > 0 && TX < t) || t < 0)
    t = TX;
end

%Get the time the ball takes to reach previous quadrant (if at all) in y
if(4 * VYIni ^ 2 + 8 * YAccel(YNumElements-QuadY+1, XNumElements-QuadX+1) * ((QuadY - 1) * YGridLen - YPos) > 0 && VYIni < 0)
TY = (-2 * VYIni + sqrt(4 * VYIni ^ 2 + 8 * (sign(VYIni) * YFric(YNumElements-QuadY+1,XNumElements-QuadX+1) +...
     YAccel(YNumElements-QuadY+1,XNumElements-QuadX+1)) *((QuadY-1)* YGridLen - YPos))) / (2 * ...
     (sign(VYIni) * YFric(YNumElements-QuadY+1,XNumElements-QuadX+1) +...
     YAccel(YNumElements-QuadY+1,XNumElements-QuadX+1)));
end

if(YAccel == zeros(YNumElements, XNumElements))
    TY = abs(((QuadY - 1) * YGridLen - YPos)/VYIni);
end
```

Code Screenshot 3

```
%update the time for calculations if it is smaller
if((TY > 0 && TY < t) || t < 0)
    t = TY;
end

%If there is an error in the time calculations, break out of the loop
if(t < 0)
    break;
end

%Update position
XPos = XPos + VXIni * t + 0.5 * XAccel(QuadY,QuadX) * t ^ 2;
YPos = YPos + VYIni * t + 0.5 * YAccel(QuadY,QuadX) * t ^ 2;
%Update Velocity
VXIni = VXIni + XAccel(QuadY,QuadX) * t;
VYIni = VYIni + YAccel(QuadY,QuadX) * t;


if(TX == t)
    XPos = round(XPos);
end

if(TY == t)
    YPos = round(YPos);
end


%Update the quadrant number
QuadX = floor(XPos / XGridLen) + 1;
QuadY = floor(YPos / YGridLen) + 1;
count = count + 1;

if(QuadX < 0)
    QuadX = 0;
end
if(QuadY < 0)
    QuadY = 0;
end

%add current position to graph array
GraphX(count) = XPos;
GraphY(count) = YPos;
color(count) = sqrt(VXIni^2 + VYIni^2);
```

Code Screenshot 4

```
    %if too many iterations are performed, break
    if (count > 1000)
        break
    end
end

%for future use
% numZero = zeros(size(GraphX));
% fin = color ./ max(color);

%contourf(sqrt(XGreenSlope.^2+YGreenSlope.^2),80,'LineStyle','none');
title('Golf Ball Displacement');
xlabel('X-Position (m)');
ylabel('Y-Position (m)');
hold on
%For future use
%surface([GraphX;GraphX], [GraphY;GraphY], [numZero;numZero],[fin;fin], 'facecol', 'no','edgecol', 'interp', 'LineWidth', 5);
plot(GraphX,GraphY,'Color',[0,0,0],'LineWidth',2)
axis([1,YGreenLen,1,XGreenLen])
```

Code Screenshot 5

REFERENCES

[1] Delay, D., Nougier, V., Orliaguet, J., and Coello, Y., 1997, "Movement Control in Golf Putting," *Human Movement Science,* Vol. 16, pp. 597-619.

[2] Sim, M., and Kim, J., 2010, "Differences Between Experts and Novices in Kinematics and Accuracy of Golf Putting," *Human Movement Science,* Vol. 29, pp. 932-946.

[3] Fernandes, O, et al, 2013 "New Technologies to the Study the Golf Putting," *Conference: Motion Analysis and Biofeedback for Improving the Performance of Golf Players,* pp. 185-191.

[4] Choi, J.S., Kim, H.S., Yi, J.H., Lim, Y.T., and Tack, G.R., 2008, "Kinematic Analysis of Golf Putting for Elite and Novice Golfers," *The Impact of Technology on Sport,* CRC Press, pp. 277-282.

[5] Shadmehr, R., and Wise, S.P., 2012. "Computational Neurobiology of Reaching and Pointing," MIT Press, Cambridge, MA.

[6] Penner, A.R., "The Physics of Putting," 2002, *Canadian Journal of Physics*, Vol. 80 No. 2, pp. 83-96.

[7] United States Golf Association, 2004, "Stimpmeter Instructional Booklet," Online Instructional Booklet, http://www.usga.org/course_care/articles/management/greens/Stimpmeter-Instruction-Booklet/.

[8] Holmes, B.W, 1986, "Dialogue Concerning the Stimpmeter," Physics Teacher, Vol 24, pp. 401-404.

[9] Brede, A.D., 1991, "Correction for Slope in Green Speed Measurement of Golf Course Putting Greens," *Agronomy Journal*, Vol. 83 No. 2, pp. 425-426.

[10] Weber, A., 1997, "Green Speed Physics," USGA Green Section Record Vol. 35 No. 2 pp. 12-15

[11] United States Golf Association, 2013, "New USGA Stimpmeter Now Available," USGA Green Section Record.

[12] Oatis, D.A., 1990, "It's Time We Put the Green Back in Green Speed," USGA Green Section Record.

[13] Gaussoin, R, Nus, J., and Leuthold, L, 1995, "A Modified Stimpmeter for Small-plot Turfgrass Research," *HortScience*, Vol 30 No 3 pp. 547-548.

[14] Domenech, A, Domenech, T, and Cebrian, J., 1987, "Introduction to the study of rolling friction," *American Journal of Physics* Vol. 55 No. 3 pp. 231-235.

[15] Kolkowitz, S, 2007, "The Physics of a Golf Putt," Coursework for Physics 210, Stanford University.

[16] Grober, R.D., 2011, "The Geometry of Putting on a Planar Surface," ARXIV, Yale University.

[17] Marquardt, C, 2007, "The SAM PuttLab: Concept and PGA Tour Data," *Annual Review of Golf Coaching*, pp. 101-114.

[18] Hill, B.P., 2010, "A Finite Element Method Study of Coefficients of Restitution in Golf Driver Clubfaces," M.S. Thesis, Rensselaer Polytechnic Institute.

[19] Magnum, G, 2008, *Optimal Putting*, Axess Book Printing, Cumming, GA.

[20] Hibbeler, R.C., “Engineering Mechanics: Dynamics, 12th Edition” Prentice Hall; Upper Saddle River, NJ.

[21] Kreyszig, E, 1999, “Advanced Engineering Mathematics, 8th Edition” Wiley, New York, NY